ROOT UV-B SENSITIVE2 Acts with ROOT UV-B SENSITIVE1 in a Root Ultraviolet B-Sensing Pathway[1][C][OA]

Colin D. Leasure[2], Hongyun Tong[2], Gigi Yuen[3], Xuewen Hou[4], Xuefeng Sun, and Zheng-Hui He*

Department of Biology, San Francisco State University, San Francisco, California 94132

Ultraviolet B light (UV-B; 280–320 nm) perception and signaling are well-known phenomena in plants, although no specific UV-B photoreceptors have yet been identified. We previously reported on the *root UV-B sensitive1* (*rus1*) mutants in Arabidopsis (*Arabidopsis thaliana*), which display a block to development under very-low-fluence-rate UV-B (<0.1 μmol m^{-2} s^{-1}) after the seedling emerges from the seed. Here, we report the analysis and cloning of the *rus2-1* mutation in Arabidopsis. The phenotype of *rus2-1* mutant seedlings is virtually indistinguishable from the phenotype of *rus1* seedlings. A map-based approach was used to clone *RUS2*. *RUS2* encodes a domain of unknown function (DUF647)-containing protein that is homologous to the RUS1 protein. *rus1-2 rus2-1* double mutant seedlings have the same phenotype as both *rus1* and *rus2* single mutants, suggesting that the two genes work in the same pathway. RUS2-Green Fluorescent Protein shows a similar expression pattern as that of RUS1-Green Fluorescent Protein, and RUS1 and RUS2 proteins interact physically in yeast. This protein-protein interaction depends on the DUF647 domain, and site-directed mutagenesis identified specific residues in DUF647 that are required for both protein-protein interaction and physiological function. Six *RUS* genes are found in Arabidopsis, rice (*Oryza sativa*), and moss (*Physcomitrella patens*), and one *RUS* member, *RUS3*, is conserved in plants and animals. Our results demonstrate that RUS2 works with RUS1 in a root UV-B-sensing pathway that plays a vital role in Arabidopsis early seedling morphogenesis and development.

The ability to perceive and respond to light, both qualitatively and quantitatively, is critically important for the survival of plants (Whitelam and Halliday, 2007). Light is well known to be important to plants for photosynthesis, but it is also used as a developmental signal and can be a source of cellular damage that plants must cope with (Lao and Glazer, 1996; Ries et al., 2000). Ultraviolet B light radiation (UV-B; 280–320 nm) can cause severe deleterious effects in biological organisms, despite representing only a small amount of total solar radiation (Caldwell et al., 1998; McKenzie et al., 2003). UV-B can cause damage to DNA by creating cyclobutane pyrimidine dimers and pyrimidine (6-4) pyrimidone dimers, which can lead to breaks and point mutations if not correctly repaired (Garinis et al., 2005). Additionally, proteins, lipids, and cellular machinery, including photosynthetic machinery, can be damaged by UV-B light (Wilson et al., 1995; Ballare et al., 1996). The amount of UV-B that an organism is exposed to can vary greatly, depending on the position of the sun in the sky and atmospheric conditions. Organisms have evolved mechanisms to perceive and adapt to changing UV-B light conditions (e.g. production of UV-absorbing compounds; Frohnmeyer and Staiger, 2003). Plants are especially vulnerable to UV-B radiation, as they have no means by which to transport themselves away from the light source/sun. Extensive research has focused on the response of plants to damaging levels of UV-B. Interestingly, in addition to damaging biological organisms, UV-B is known to have some positive effects. Plants also have some well-documented photomorphogenic responses to UV-B light (Nogues et al., 1999; Suesslin and Frohnmeyer, 2003; Ulm and Nagy, 2005), although as yet no receptors have been identified in plants for UV-B wavelengths.

Although many genes have been found to be regulated by UV-B in plants, a specific receptor has yet to be identified (Ulm et al., 2004; Brown et al., 2005). The difficulty in identifying the UV-B receptor arises in part from the difficulty in separating the response to

[1] This work was supported by the National Science Foundation (Faculty Early Career Development [CAREER] Program award no. MCB9985185) and the National Institutes of Health (Support of Competitive Research [SCORE] Institutional Development award no. S06 GM52588) to Z.-H.H.

[2] These authors contributed equally to the article.

[3] Present address: Genentech, Inc., 1 DNA Way, South San Francisco, CA 94080.

[4] Present address: Laboratory of Molecular Plant Physiology, College of Life Sciences, South China Agricultural University, Guangzhou 510642, China.

* Corresponding author; e-mail zhe@sfsu.edu.

The author responsible for distribution of materials integral to the findings presented in this article in accordance with the policy described in the Instructions for Authors (www.plantphysiol.org) is: Zheng-Hui He (zhe@sfsu.edu).

[C] Some figures in this article are displayed in color online but in black and white in the print edition.

[OA] Open Access articles can be viewed online without a subscription.

www.plantphysiol.org/cgi/doi/10.1104/pp.109.139253

UV-B light itself from the response to the damage caused by UV-B light. In animals, it is known that UV-B perception can occur via the interconversion of one form of a molecule into another upon UV-B absorption (e.g. cis-urocanic acid and 6-formylindolo[3,2-b]carbazole; Walterscheid et al., 2006; Fritsche et al., 2007). It is not known if plants use similar UV-B perception mechanisms or have evolved a unique mechanism(s). Plants have multiple photoreceptors for the perception of red/far-red light (Quail et al., 1995; Smith, 1999; Bae and Choi, 2008) and blue/UV-A light (Cashmore et al., 1999; Liscum et al., 2003; Christie, 2007). All of these wavelengths are extremely important for plants, as they provide vital clues about their light environment in addition to being used as the energy source for photosynthesis. Additionally, specific photomorphogenic responses to UV-B suggest that a specific photoreceptor exists in plants for perceiving the UV-B light itself and not just the damage caused by UV-B light (Ulm and Nagy, 2005).

In plants, UV-B is known to elicit certain photomorphogenic responses, including inhibition of hypocotyl elongation and root growth (Kim et al., 1998), cotyledon opening (Ulm and Nagy, 2005), stomatal closure (Nogues et al., 1999), and anatomical changes associated with UV-B protection, such as increased epicuticular wax (Steinmüller and Tevini, 1985) and decreased leaf surface size. Many genes in Arabidopsis (*Arabidopsis thaliana*) have been found to have their expression regulated by UV-B, including genes such as *CHALCONE SYNTHASE* and *ELONGATED HYPOCOTYL5* (*HY5*; Ulm et al., 2004). The CHALCONE SYNTHASE enzyme acts at a regulatory step in the production of anthocyanin and other flavonoids that serve as important plant photoprotection pigments. The F-box protein CONSTITUTIVELY PHOTOMORPHOGENIC1 regulates transcriptional factors such as HY5 and HY5-HOMOLOG (HYH) that are involved in UV-B responses (Oravecz et al., 2006). Mutants affecting the production of UV-B-protecting flavonoids make plants more sensitive to the damaging effects of UV-B (Li et al., 1993). The photolyase responsible for repairing cyclobutane pyrimidine dimers is also upregulated by UV-B light (Waterworth et al., 2002). Much of the previous research into the UV-B response in plants has focused on high fluence (>1 μmol m^{-2} s^{-1}) levels of UV-B, levels generally considered damaging. Signaling pathways stimulated by low-fluence (LF; 0.1–1.0 μmol m^{-2} s^{-1}) and very-low-fluence (VLF; <0.1 μmol m^{-2} s^{-1}) UV-B signals likely represent the nondamaging photomorphogenic response.

The duplication and divergence of genes is an important phenomenon in the evolution of species (Taylor and Raes, 2004). Frequently, duplicated proteins will diverge in sequence and function and still interact with their duplicated paralog to form heterodimers or heteromultimers with new functions (Ispolatov et al., 2005). Examples of this in Arabidopsis are commonplace and have been well characterized for protein families such as MADS domain-containing transcription factors (Riechmann et al., 1996), Auxin Response Factor/Indole-3-Acetic Acid interactions (Ulmasov et al., 1999), and countless receptor kinase dimerizations (e.g. BRI1 [Russinova et al., 2004] and CLV1/2 [DeYoung and Clark, 2001]). This type of evolution is a powerful way for protein complexes to diversify and fine-tune their functions in ways that would not be possible with only a single gene.

We previously identified a mutant, *root UV-B sensitive1* (*rus1*), that under LF to VLF UV-B light displayed a severe developmental arrest after germination (Tong et al., 2008). The RUS1 protein contains a conserved domain of unknown function (DUF), listed as DUF647. Here, we report the identification and cloning of the *RUS2* gene that also encodes a DUF647-containing protein. Our genetic and biochemical analyses suggest that RUS2 works together with RUS1 in Arabidopsis root UV-B-sensing pathways.

RESULTS

rus2-1 Mutant Seedling Development Is Blocked by UV-B Light

rus2-1 mutant plants display a stall in development after the radicle and cotyledons have emerged from the seed (Fig. 1A). Cotyledons fail to green fully, the root does not elongate, and the development of true leaves is greatly delayed. Interestingly, *rus2-1* plants recover when transplanted from Murashige and Skoog (MS) medium petri dishes into soil and also grow much better when sown directly onto soil. One major difference between the environments of the soil and the petri dish is the amount of light that the roots of the plants receive. We hypothesized that the light exposure difference between the soil and the MS medium plates affects the phenotype of the *rus2-1* mutant plants. We observed that when the roots of *rus2-1* mutants are covered, even on MS plates, the *rus2* phenotype is partially alleviated and the plants develop more like wild-type plants (Fig. 1, B and C).

To analyze the role of light in the mutant phenotype of *rus2-1* plants, we cut the relative amount of light to these plants by the use of neutral density (ND) filters (Fig. 1A). Standard growth chamber fluorescent lights were used as the light source. MS medium plates were covered by the ND filters to reduce the total light intensity. The total photosynthetically active radiation (PAR) for each condition is shown in Table I. We previously analyzed the ND filters and found that they reduced the amount of light across all wavelengths (Tong et al., 2008). In this experiment, we grew *rus2-1* seedlings alongside wild-type ecotype Columbia (Col) seedlings. We measured the amount of root growth for 7-day-old Col and *rus2-1* seedlings under decreased total PAR conditions. As total PAR was reduced, the *rus2-1* seedling root length increased (Table I). The lowered light intensities did not dramatically affect the wild-type control, although there was a slight increase

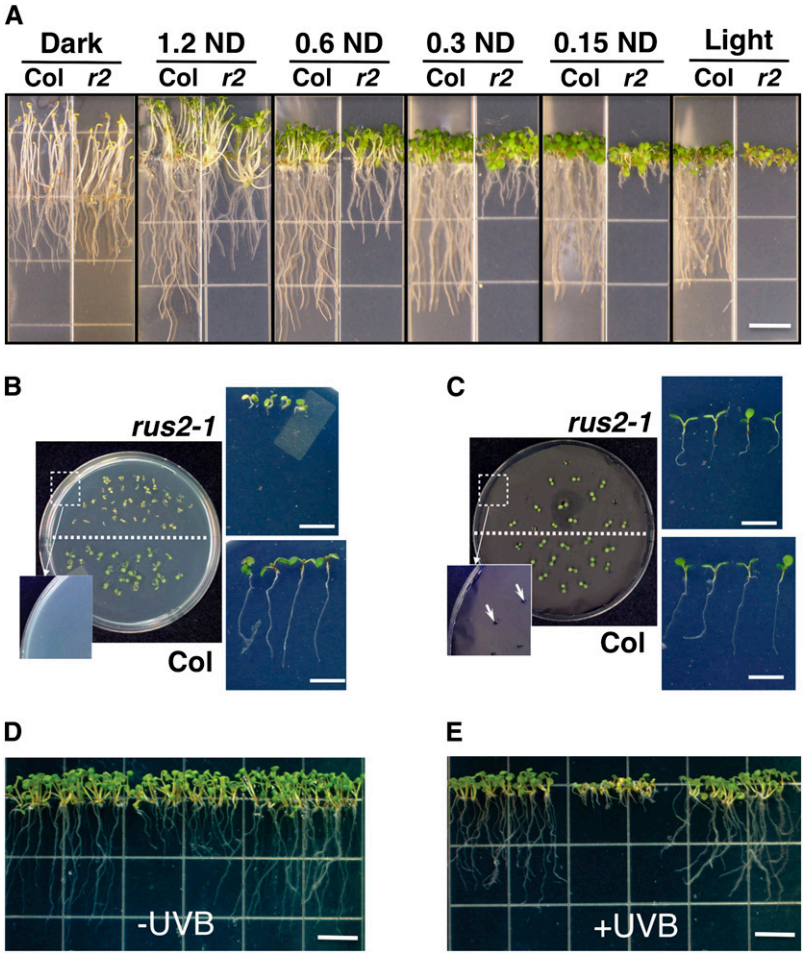

Figure 1. *rus2-1* is hypersensitive to UV-B. A, Growth of wild-type (Col) and *rus2-1* (*r2*) plants under various light conditions created by ND filters (1.2, four stop; 0.6, two stop; 0.3, one stop; 0.15, one-half stop). Bar = 1 cm. B, *rus2-1* and wild-type (Col) plants grown horizontally on an uncovered MS medium petri dish. Representative plants were removed and imaged vertically in the panels to the right. A closeup view of the medium surface is shown in the inset. Bars = 1 cm. C, *rus2-1* and wild-type (Col) plants grown horizontally on a black foil-covered MS medium petri dish. A closeup view of the medium surface is shown in the inset. Holes (0.4 mm diameter) were generated on black foil to allow seeds to contact growth medium (arrows). Representative plants were removed and imaged vertically in the panels to the right. Bars = 1 cm. D and E, Wild-type (Col), *rus2-1*, and *rus2-1;pAt2g31190::At2g31190-GFP* plants grown in a UV-B-reduced environment (−UV-B; covered by Photodyne UV filter, a UV-B-absorbing plastic) or a normal growth chamber environment (+UV-B; covered by transparent plexiglass acrylic sheet, a UV-B-transmitting plastic). Bars = 1 cm. [See online article for color version of this figure.]

in root length of the wild type as light intensities were reduced. Etiolated *rus2-1* seedlings were very similar in this experiment to the wild-type, with an average root length 82.6% that of the wild type (Table I). This experiment shows that the severity of the *rus2-1* phenotype is directly related to the intensity of light exposure.

rus2-1 mutant plants grown on MS medium plates with exposed roots recover considerably when transferred to soil, an environment where the roots are covered (see Fig. 4A below). Therefore, we hypothesized that the location of light perception responsible for the *rus2-1* mutant phenotype is the root. To test this hypothesis, we covered the surface of MS medium plates with black metal foil with pinholes through which the roots could grow. The black surface reduces the amount of light that the roots are exposed to while allowing the apical portions of the plant to be exposed to the normal amount of light. *rus2-1* plants grown horizontally on the uncovered control plate displayed a strong phenotype (Fig. 1B, top). *rus2-1* seedlings grown horizontally on black metal foil-covered plates showed elongated roots and greener apical portions/cotyledons (Fig. 1C, top). This result suggests that the light environment of the root elicits not only the *rus2-1* root phenotype but also the shoot phenotype.

Growth of *rus2-1* plants on monochromatic light sources (blue light-emitting diode, λ maximum emission of 470 nm; green light-emitting diode, λ maximum emission of 525 nm; red light-emitting diode, λ maximum emission of 633 nm) showed that none of the canonical light perception wavelengths (320–750 nm) is able to elicit the strong *rus2-1* phenotypes (data not shown), a phenomenon found in *rus1* (Tong et al., 2008). Additionally, *rus2-1* double mutants with *phototropin*, *phytochrome A*, *phytochrome B*, and *cryptochrome* mutants (*phot1*, *phot2*, *phot1phot2*, *nph3*, *phyA*, *phyB*, *phyAphyB*, *cry1*, *cry 2*, *cry1cry2*) still displayed the same *rus* mutant phenotype (data not shown). Therefore, we hypothesized that UV-B light was responsible for the *rus2* phenotype. To test this hypothesis, we covered plates in our growth chamber with either a UV shield or a sheet of non-UV-absorbing plastic as a control. Under the UV-B shield conditions, the *rus2-1* mutant plants recovered considerably, reaching roughly half the root length of the wild-type plant (Fig. 1D). The non-UV-absorbing plastic-covered control plates did not show any recovery of the *rus2-1* phenotype (Fig. 1E). This result suggests that UV-B is predominantly responsible for the mutant phenotypes in the *rus2-1* mutant. We measured a UV-B fluence rate of 0.300 μmol m^{-2} s^{-1} in the normal light conditions in our

Table I. *Effect of fluence rates on rus2 root development*

Filter Condition	Light Measurement		Root Length (n = 30)		
	PAR	UV-B			
	$\mu mol\ m^{-2}\ s^{-1}$			mm ± SE	% of wild type
No filter (light)	71.2	0.300	Wild type	25.47 ± 0.91	4.7
			rus2	1.18 ± 0.04	
Lee ND 298 (0.15, one-half stop)	47.8	0.177	Wild type	28.60 ± 1.19	17.9
			rus2	5.12 ± 0.17	
Lee ND 209 (0.3, one stop)	39.2	0.077	Wild type	30.38 ± 0.93	31.1
			rus2	9.45 ± 0.13	
Lee ND 210 (0.6, two stop)	18.8	0.055	Wild type	29.16 ± 1.12	42
			rus2	12.24 ± 0.55	
Lee ND 299 (1.2, four stop)	4.73	0.025	Wild type	29.08 ± 1.72	56.9
			rus2	16.55 ± 0.93	
No filter (dark)	0	0	Wild type	15.88 ± 0.52	82.6
			rus2	13.12 ± 0.30	

growth chamber (Tong et al., 2008). Of the ND filters that we used, the one with the highest reduction in light intensity (ND 0.15) had a UV-B fluence rate of 0.025 μmol m^{-2} s^{-1}. Even in the ND-0.15 light conditions, a partial *rus2-1* phenotype was observed. Thus, we conclude from our data that LF and VLF UV-B can elicit the *rus2-1* phenotype.

Cloning and Identification of the *rus2-1* Mutation

The *rus2-1* mutation was identified from a screen for *rus*-like phenotypes using fast-neutron mutagenesis (Koornneef et al., 1982). To map the mutation, we crossed a *rus2-1* plant with a wild-type Landsberg *erecta* plant, allowed the F1 generation plants to self-fertilize, and collected F2 seeds. Using cleaved amplified polymorphic sequence (Konieczny and Ausubel, 1993) and simple sequence length polymorphism genetic markers, we rough mapped the *rus2-1* mutation to near the marker VE017, which is on the southern arm of chromosome II (Fig. 2A). We used cleaved amplified polymorphic sequence and simple sequence length polymorphism markers to fine-map the mutation to a region on bacterial artificial chromosome (BAC) F16D14 (Fig. 2A). As fast-neutron mutagenesis can cause large lesions in DNA, we PCR amplified several genes in this region as a quick attempt to find altered PCR product lengths that might represent the *rus2-1* mutation. In the *rus2-1* background, we were unable to amplify the full-length *At2g31190* gene, despite being able to use the same primer pairs to amplify this gene in the wild-type background. To complement the *rus2-1* mutant phenotype, we cloned the *At2g31190* gene in frame with the *GFP* coding sequence and transformed *rus2-1* mutant plants. The *At2g31190-GFP* transgene completely complements the *rus2-1* mutant phenotype in planta (Figs. 1, D and E, and 2G).

To identify the nature of the *rus2-1* mutation, we attempted to PCR amplify overlapping portions of *At2g31190* for sequencing. Although we could amplify regions at the end of the gene, we failed to amplify internal portions of the gene in the *rus2-1* background, despite being able to amplify these same fragments from the wild type. Additionally, we were unable to amplify across the entire length of the gene, something that should be possible with a simple deletion. These results suggested that the mutation was the result of a chromosomal rearrangement. We determined the exact nature of the *rus2-1* mutation using thermal asymmetric interlaced PCR (Liu and Huang, 1998), working from both ends of the gene toward the middle. Thermal asymmetric interlaced PCR showed that the *rus2-1* mutation is a disruption in the last intron and that the chromosome was broken there and reattached incorrectly to another portion of chromosome II (Fig. 2B). Our results indicate that two break points occurred in chromosome II and were repaired in a reverse orientation (Fig. 2C, red portion). The second break point is on BAC T1B3 after bp 15,812, in a region where no genes are predicted to occur (Swarbreck et al., 2008). At these two break point/repair sites, no genomic DNA was deleted, and a single T/A base pair was added at each site (Fig. 2, D and E, underlined base). Primers spanning either of the two break point sites yielded products only in the wild type (Fig. 2F). Recombining the same set of primers amplified mutant T1B3-*RUS2* pieces as predicted (Fig. 2F). Reverse transcription (RT)-PCR analysis showed no expression of *RUS2* after the break point (Fig. 2G). As the *At2g31190* gene is disrupted in the *rus2-1* background and capable of fully complementing the *rus2-1* phenotype (Fig. 2G) in more than six independent lines, we conclude that *RUS2* is *At2g31190*.

RUS2 Encodes a DUF647-Containing Protein

RUS2 encodes a 433-amino acid protein (48 kD) with no known function(s). A BLAST search with the RUS2 protein sequence uncovered the presence of an evolutionarily conserved domain called DUF647 (Pfam accession no. PF04884) in this protein. Additionally, the

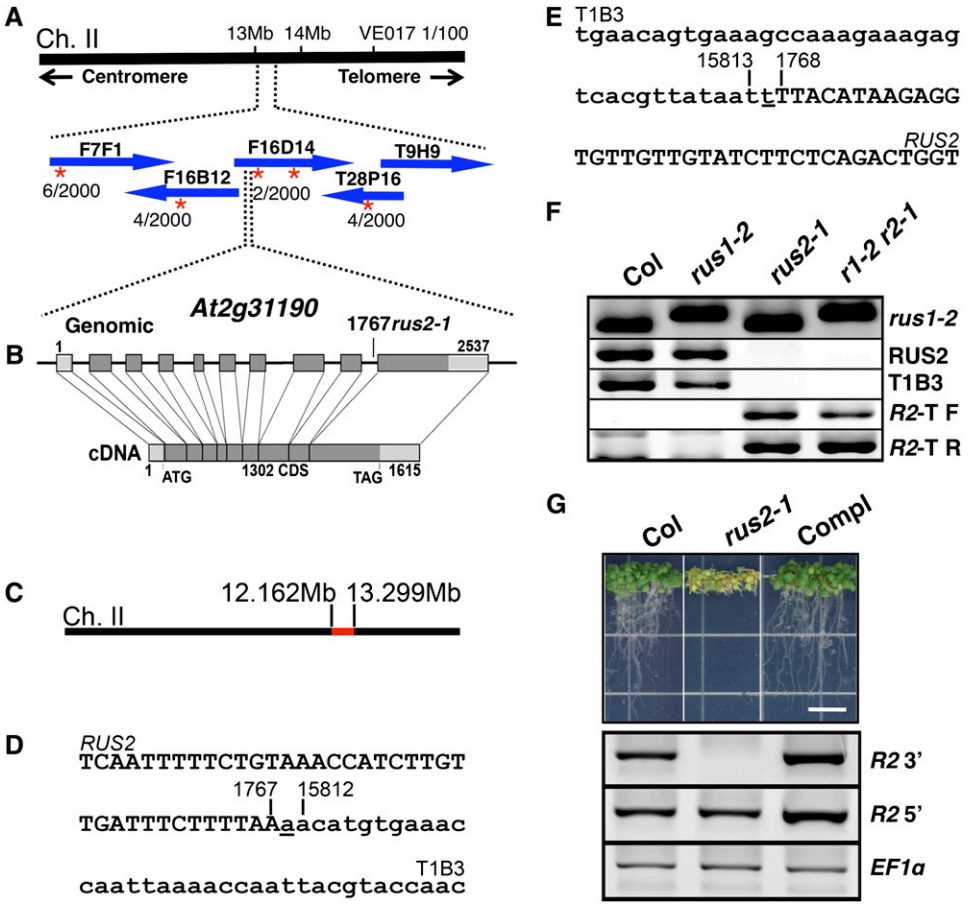

Figure 2. *rus2-1* mapping and complementation. A, Genomic region of chromosome II containing the *RUS2* (*At2g31190*) gene. B, Illustration of the genomic structure and the resulting cDNA for the *RUS2* gene. Numbers indicate the start/end positions of At2g31190 (genomic, top; cDNA, bottom). C, Illustration of chromosome II with the inverted region in the *rus2-1* mutation shown in red. Numbers represent approximate chromosomal positions of the two break points. D and E, Sequence around the *RUS2*-T1B3 fusion junctions. *RUS2* sequences are in uppercase. T1B3 sequences are in lowercase. The inserted T/A base pair is in underlined lowercase. Numbers correspond to positions relative to the start of the *RUS2* cDNA or the position on the T1B3 BAC. F, Genotyping of wild-type (Col), *rus1-2*, *rus2-1*, and *rus1-2 rus2-1*(*r1-2 r2-1*) plants for *rus1-2* (first row) and *rus2-1* (second to fifth rows). PCR results of primers across the insertion/deletion site (net +44 bp) in *rus1-2* mutants are shown (*rus1-2* row). The larger band represents the *rus1-2* mutation. The *RUS2* row shows the PCR result of primers spanning the *RUS2* break point site. The T1B3 row shows the PCR result of primers spanning the T1B3 break point site. The *R2*-T F row shows the PCR result of the forward primers from *RUS2* and T1B3. The *R2*-T R row shows the PCR result of the reverse primers from *RUS2* and T1B3. G, Complementation of *rus2-1* and *RUS2* expression. The top panel shows vertically grown wild-type (Col), *rus2-1*, and *rus2-1* transgenic plants carrying *pRUS2*::*RUS2-GFP* (Compl). The bottom panel shows *RUS2* gene expression in wild-type (Col), *rus2-1*, and *rus2-1* transgenic plants carrying *pRUS2*::*RUS2-GFP* (Compl). Primers after the *rus2-1* break point mutation (*R2* 3′) and before the *rus2-1* break point mutation (*R2* 5′) were used. *EF1α* was used as a control. Bar = 1 cm. [See online article for color version of this figure.]

RUS2 protein is annotated by The Arabidopsis Information Resource (www.arabidopsis.org; Swarbreck et al., 2008) and National Center for Biotechnology Information databases as containing a DUF647 from amino acids 50 to 433. Thus, both RUS1 and RUS2 share the DUF647 domain, and mutations in either of the two genes produce very similar, if not identical, phenotypes. Two-protein BLAST alignments show that RUS1 and RUS2 are 28% identical and 49% similar across the conserved region of the proteins. The conserved regions of RUS1 (amino acids 200–536) and RUS2 (amino acids 73–385) essentially correspond to the DUF647 domain. Therefore, we conclude that RUS2 and RUS1 are DUF647-containing homologs with similar mutant phenotypes. There is no predicted sequence similarity for the regions of the two proteins preceding the homologous regions.

RUS2 Is Most Strongly Expressed in the Root Tip

In order to ascertain the location of the RUS2 protein in vivo, we cloned the *RUS2* gene, including promoter,

in frame with the *GFP* coding sequence. This construct fully complements the *rus2-1* phenotype (Figs. 1, D and E, and 2G). When visualized by confocal light scanning microscopy, we detected a low level of GFP fluorescence (Fig. 3E) in the root tip that was consistently higher than the background autofluorescence of the wild-type controls (Fig. 3B). The GFP fluorescence in the root tip is strikingly similar to the localization we previously reported for the RUS1 protein (Tong et al., 2008). RUS2-GFP does not appear to be localized to the cell wall or specifically to the nucleus. Despite only observing RUS2-GFP in the root tip, we cannot rule out that RUS2-GFP is present in other tissues at levels below detection. In fact, RT-PCR data for *RUS2* expression suggests that *RUS2* is expressed throughout the plant at a relatively uniform level (see Fig. 6B below). Additionally, genechip data obtained from the Genevestigator resource is consistent with our analyses, as it reports *RUS2* expression throughout the plant body, with about a 4-fold increase in *RUS2* expression in the root tip as compared with other parts of the root (www.genevestigator.ethz.ch; Zimmermann et al., 2004). Thus, *RUS2* transcript is expressed throughout the plant, with strongest expression in the root tip, the region affected most strongly in the *rus2-1* phenotype.

We analyzed the RUS2 protein sequence using the target signal prediction programs WoLF PSORT (www.wolfpsort.org; Horton et al., 2006, 2007) and TargetP 1.1 (http://www.cbs.dtu.dk/services/TargetP; Emanuelsson et al., 2000). Neither of these programs predicts a strong subcellular localization for RUS2. A previous well-conducted proteomic study found the RUS2 protein in purified plastid extracts (Ferro et al., 2003). This is consistent with our GFP fusion results, which show that RUS2 is not in the cell wall or membrane and is not localized to the nucleus. Additionally, WoLF PSORT and TargetP 1.1 predict that the RUS1 protein is localized to the plastid and that RUS1-GFP shows virtually the identical GFP fluorescence pattern as RUS2-GFP. Thus, our data here are consistent with the empirical results reported before, which show RUS2 to be in the chloroplast (Ferro et al., 2003).

rus2-1 Interacts Genetically with the *rus1-2* Mutation

We previously reported the characterization and cloning of the *rus1* mutations and their effects on Arabidopsis seedlings grown under UV-B light (Tong et al., 2008). The *rus2-1* mutation was identified in the same screen as the *rus1-1* and *rus1-2* mutations. Early in our analyses, we noted the striking similarities between *rus1* mutants and the *rus2* mutant described here. To analyze the genetic relationship between these two genes, we crossed a *rus2-1* plant with a *rus1-2* plant. We used *rus1-2* in this cross as it is equally as strong as the *rus1-1* and *rus1-3* alleles and it is in the same genetic background as *rus2-1* (Col; wild-type *GLABROUS*; Tong et al., 2008). Offspring in the F1 generation were phenotypically normal, suggesting that the *rus1-2* and *rus2-1* mutations are not affecting the same gene (data not shown). Due to the severity of these mutants, we hypothesized that the double *rus1 rus2* mutant would be even more severe, possibly even embryo lethal. To create a double mutant, we allowed the *rus1-2/+ rus2-1/+* F1 plants to self-fertilize and collected seeds for the F2 generation. From the F2 generation, we found a plant that was homozygous for both the *rus1-2* and *rus2-1* mutations and collected F3 seeds for further analysis.

When grown vertically on MS medium plates under our normal growth chamber light conditions (71.2 μE, PAR), the *rus1-2 rus2-1* double mutant appears indistinguishable from both the *rus1-2* and *rus2-1* single mutants (Fig. 4A). In the light, the double mutant germinates and arrests at the same time as either of the single mutants. On MS agar plates, the roots of 7-d-old light-grown *rus1-2 rus2-1* double mutant seedlings

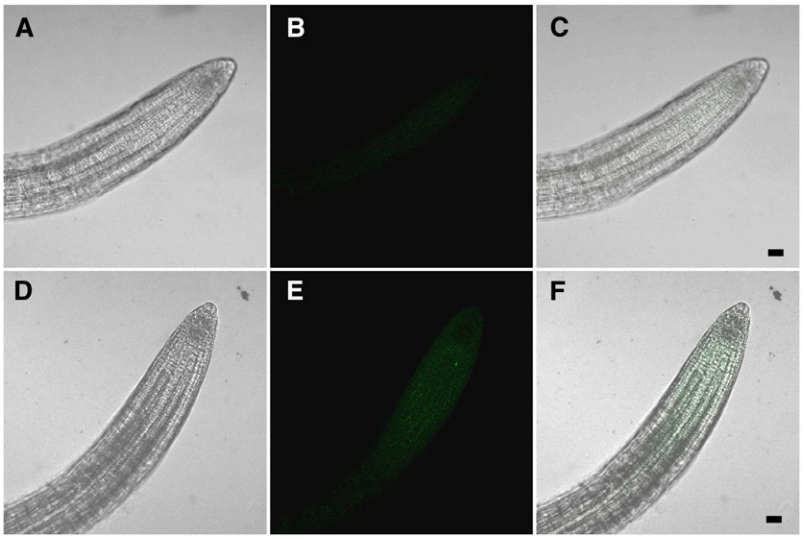

Figure 3. RUS2 is expressed in roots. A, Bright-field image of a wild-type root. B, Background fluorescence of a wild-type root. C, Merged image of A and B. D, Bright-field image of transgenic RUS2::RUS2-GFP roots. E, GFP fluorescence of transgenic RUS2::RUS2-GFP roots. F, Merged image of D and E. Bars = 10 μm.

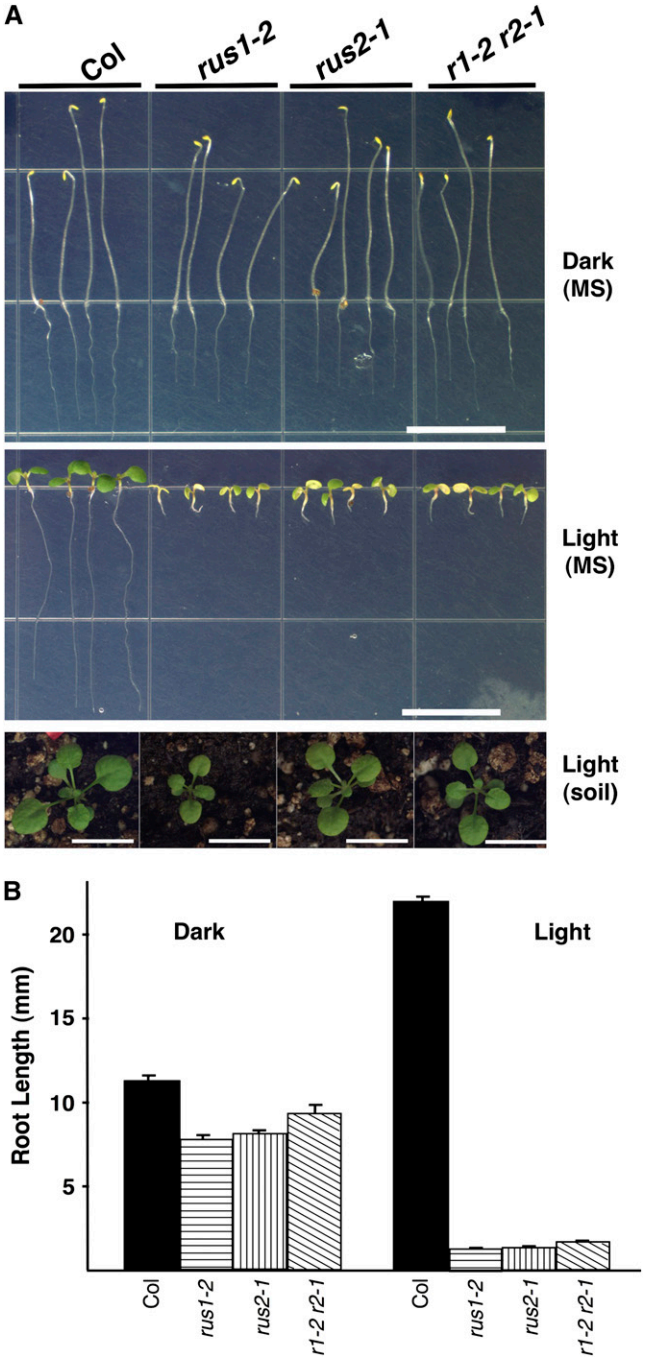

Figure 4. Phenotypic analysis of *rus1* and *rus2* single mutants and the *rus1 rus2* double mutant. A, Dark-grown (top) and light-grown (middle) wild-type (Col), *rus1-2*, *rus2-1*, and *rus1-2 rus2-1* (*r1-2 r2-1*) plants are shown. Seedlings were grown vertically for 7 d on MS plates. The bottom panel shows wild-type (Col), *rus1-2*, *rus2-1*, and *rus1-2 rus2-1* (*r1-2 r2-1*) plants that were grown for 7 d on a plate and then transferred to soil for 12 d. Representative single plants from each line are shown. Bars = 1 cm. B, Graph of average root lengths in dark- or light-grown wild-type (Col), *rus1-2*, *rus2-1*, and *rus1-2 rus2-1* (*r1-2 r2-1*) plants. n = 12 for all genotypes/light conditions. Error bars represent SE. [See online article for color version of this figure.]

were of a comparable length to either of the single mutants (Fig. 4B, Light). We next examined 7-d-old etiolated (dark-grown) seedlings for the wild type, *rus1-2*, and *rus2-1* single mutants and the *rus1-2 rus2-1* double mutant (Fig. 4A). The roots of *rus1-2 rus2-1* double mutants greatly elongated in the dark, as compared with the roots of *rus1-2 rus2-1* light-grown seedlings. The roots of the single and double mutants grew to about 75% that of the wild type in the dark. These results support a rejection of our initial hypothesis that the *rus1-2 rus2-1* double mutant plants would be more severe than either single mutant alone. Instead, these data suggest that *RUS1* and *RUS2* are both part of the same genetic pathway and are likely to function in the same biochemical pathway. A loss of either *RUS1* or *RUS2* eliminates the function of this pathway, so that a further loss of the other gene has little to no effect.

RUS1 and RUS2 Interact in Yeast

As noted earlier, *rus1* and *rus2* single mutants have virtually identical phenotypes and the double *rus1 rus2* mutant has a phenotype very similar to either of the single mutants alone. Therefore, *rus1* and *rus2* mutants genetically interact in a way that strongly suggests that *RUS1* and *RUS2* are working in the same pathway. Additionally, the RUS2-GFP fluorescence pattern is very similar to the RUS1-GFP fluorescence pattern. As the RUS1 and RUS2 proteins share a similar domain, we hypothesized that these proteins interact physically. In our experiences, RUS1 and RUS2 proteins are highly unstable in vitro and rapidly degrade, even in the presence of SDS, protease inhibitors, and a reducing agent (data not shown). This characteristic of the RUS1 and RUS2 proteins made our in vitro analyses of these proteins unsuccessful. Therefore, we utilized a yeast-two-hybrid system to test for interactions between these proteins in an in vivo assay using various combinations of the RUS1 and RUS2 proteins to test our hypothesis. We used the pGADT7 and pGBKT7 vectors to create C-terminal fusions with the Gal4 activating domain (AD) and Gal4 DNA-binding domain (BD), respectively. Neither the RUS1-BD nor the RUS2-BD construct was self-activating when cotransformed with an empty AD vector (Fig. 5C; data not shown). We did not observe any self-interaction for RUS1 or RUS2 in our system (Fig. 5C). In support of our original hypothesis, we did observe interaction between RUS1 and RUS2 (Fig. 5C).

Specific Residues in the DUF647 Domain Are Required for RUS1-RUS2 Physical Interactions and Functionalities

We next hypothesized that the interaction between RUS1 and RUS2 was via the DUF647 domain. We created constructs for RUS1 that contained either the DUF647 domain (R1DUF) or the region of the protein preceding the DUF647 domain (R1preDUF). The R1DUF corresponds to amino acids 182 to 608, and

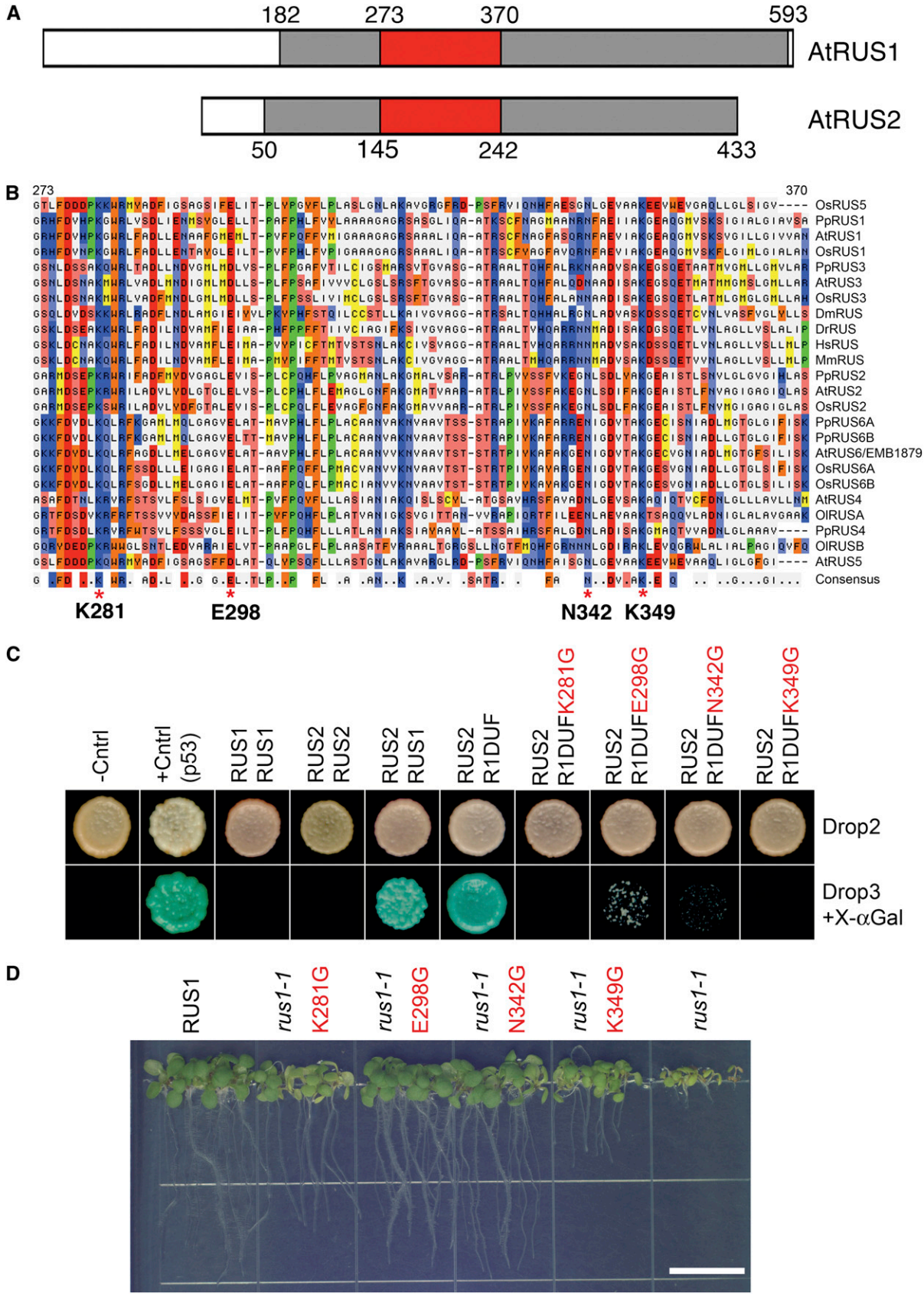

Figure 5. (*Legend appears on following page.*)

the R1preDUF corresponds to amino acids 1 to 181. R1DUF was able to interact with RUS2, and R1preDUF647 did not show any interaction with RUS2 (Fig. 5C; data not shown). The RUS2 protein has only about 50 amino acids before its DUF647 domain; thus, RUS2 is almost entirely a DUF647 domain already. Therefore, we obtained strong evidence that the DUF647 domain has a protein-protein interaction function and is required for the interaction of RUS1 with the RUS2 protein. Next, we used site-directed mutagenesis on the RUS1-AD constructs to alter four selected conserved (100% in DUF647 domains from various species) amino acids in the DUF647 domain (Fig. 5B). Two of these mutant rus1 proteins (K281G and K349G) failed to interact with RUS2 in our yeast two-hybrid system (Fig. 5C). The other two mutant rus1 proteins (E298G and N342G) interacted with RUS2, but the observed interaction was much weaker than that with the wild type (Fig. 5C). We created *pRUS1*::*RUS1* constructs with these same point mutations and transformed them into *rus1-1* mutant plants. We observed at least partial rescue of the *rus1-1* phenotype with all of these mutant constructs (Fig. 5D). Interestingly, the amount of rescue was greater in the two mutants that showed partial interaction via yeast two-hybrid assay (Fig. 5D). The fact that these mutant proteins can at least partially suppress the *rus1-1* phenotype in vivo is evidence that the mutant versions are being produced. The ability of the non-yeast two-hybrid-interacting mutants to partially suppress the *rus1-1* phenotype suggests that there are additional factors in the plant that support the function of the RUS1/RUS2 complex. Thus, these data strongly support the hypothesis that RUS1 and RUS2 physically interact via the DUF647 domain and that this interaction is important for their function in vivo.

DUF647 Proteins Exist in Many Plant, Animal, and Fungal Species

We searched the completed Arabidopsis genome and found a total of six DUF647-encoding genes (*RUS* genes; Arabidopsis Genome Initiative, 2000; Swarbreck et al., 2008). We named the additional *RUS* genes based on their genomic positions: *RUS3* (*At1g13770*), *RUS4* (*At2g23470*), *RUS5* (*At5g01510*), and *RUS6/EMB1879* (*At5g49820*). The rice (*Oryza sativa*; Goff et al., 2002; Yu et al., 2002) and moss (*Physcomitrella patens*; Rensing et al., 2008) genomes also had six *RUS* genes each. We named the rice and moss genes based on their similarity to Arabidopsis *RUS* genes as follows: *OsRUS1* (*04g22360*), *OsRUS2* (*Os04g43690*), *OsRUS3* (*Os03g11500*), *OsRUS5* (*Os01g04860*), *OsRUS6A* (*Os01g66350*), *OsRUS6B* (*Os05g34650*), *PpRUS1* (*Phypa_116804*), *PpRUS2* (*Phypa_185242*), *PpRUS3* (*Phypa_183447*), *PpRUS4* (*Phypa_161943*), *PpRUS6A* (*Phypa_209284*), and *PpRUS6B* (*Phypa_211695*). Phylogenetic analyses of the six RUS protein sequences from Arabidopsis, rice, and moss revealed large orthology among these proteins in these species. Clear orthologous clades exist for RUS1, RUS2, RUS3, and RUS6 in these species (Fig. 6A). Relationships for RUS4 and RUS5 were less strongly supported in our analysis (Fig. 6A). None of the six Arabidopsis RUS proteins appears to be the result of a lineage-specific duplication (Fig. 6A). This can be concluded because all six of the Arabidopsis RUS proteins have an obvious ortholog in rice, moss, or both that is more similar to it than any of the other five Arabidopsis RUS proteins. *RUS6/EMB1879* (www.seedgenes.org; Tzafrir et al., 2003), previously identified as an embryo-lethal gene, is duplicated in both rice and moss but not in Arabidopsis. *RUS4* appears to have been lost in rice, and *RUS5* appears to have been lost in moss, although the topology is not as strongly defined for these gene products as for the other four. To analyze the expression of the *RUS* genes in Arabidopsis, we performed RT-PCR on RNA collected from various tissues and developmental time points of wild-type plants. We observed expression of all six *RUS* genes in all of our samples (Fig. 6B).

We next looked for *RUS* genes in the completed animal genomes by BLAST search with the RUS1 protein. We found a single *RUS* gene in each of the human, mouse, *Drosophila*, zebrafish, pufferfish, horse, and cow genomes. Interestingly, we were unable to identify a *RUS* homolog in the chicken genome (*Gallus gallus*), despite using multiple search methods. The Mouse Genome Database lists *MmRUS* (*BC017158*) cDNAs from various tissues, including heart, spleen, bone marrow, dendritic cells, salivary gland, melanoma, and mammary gland tumors (www.informatics.jax.org; Eppig et al., 2007). Genechip data from Gene-

Figure 5. Interactions between RUS1 and RUS2 are required for functionality. A, Diagram illustrating the positions of the aligned sequences shown in B (red region) and the entire DUF647 (gray regions, including the red region) in AtRUS1 and AtRUS2. B, ClustalW alignment of DUF647 domain-containing proteins corresponding to amino acids 273 to 370 of AtRUS1. Amino acid substitutions used in B are shown at the bottom with asterisks. At, *Arabidopsis thaliana*; Dm, *Drosophila melanogaster*; Dr, *Danio rerio*; Hs, *Homo sapiens*; Mm, *Mus musculus*; Ol, *Ostreococcus lucimarinus*; Os, *Oryza sativa*; Pp, *Physcomitrella patens*. C, Yeast two-hybrid assay of interactions between RUS1 and RUS2. Growth of various paired AD (left) and BD (right) combinations on Drop2 and Drop3 media containing 5-Bromo-4-chloro-3-indolyl-α-D-galactoside (X-αGal). RUS1 and RUS2 are in the form of full-length fusions. R1DUF refers to the RUS1 DUF647 domain only. Site-directed mutagenesis-derived point amino acid substitutions are shown in red following R1DUF. AD-RecT was used with either BD-Lam (−Cntrl) or BD-p53 (+Cntrl) for negative and positive controls, respectively. D, Representative lines of *rus1-1* mutants transformed with either wild-type *RUS1* (RUS1) or mutant versions of *rus1* (*rus1*; with specific point mutations in red) under the native *RUS1* promoter. Untransformed *rus1-1* seeds are shown as a reference. Bar = 1 cm.

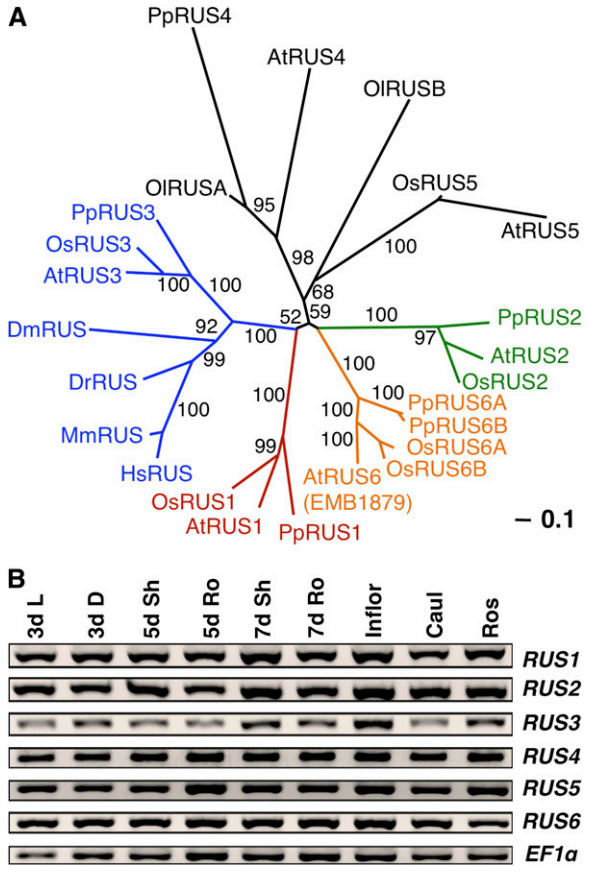

Figure 6. Phylogeny of the RUS family and expression of RUS genes in Arabidopsis. A, Phylogenetic analysis of full-length RUS proteins from various species. Bootstrap percentages are listed on each branch (1,000 replicates, rounded to the nearest percentage). Orthologous clusters are shown in different shade levels. Species abbreviations are as in Figure 5. B, RT-PCR results for the six *RUS* genes in Arabidopsis. 3d L, Three-day-old light-grown seedlings; 3d D, 3-d-old dark-grown seedlings; 5d Sh, 5-d-old light-grown seedling shoots; 5d Ro, 5-d-old light-grown seedling roots; 7d Sh, 7-d-old light-grown seedling shoots; 7d Ro, 7-d-old light-grown seedling roots; Inflor, mature inflorescence tissue; Caul, mature cauline leaf tissue; Ros, mature rosette leaf tissue. [See online article for color version of this figure.]

Note (bioinfo2.weizmann.ac.il) shows expression of *HsRUS* (*C16orf58*) at a similar level in all tissues tested. Thus, *RUS* genes do not appear to be expressed in specific tissues in the organisms for which expression data exists.

Various fungal species have RUS proteins, but the relationship to plant or animal RUS proteins is not clear and some fungi, such as *Saccharomyces cerevisiae* do not have any RUS proteins. This lack shows that it is possible for some eukaryotes to live without RUS protein(s), although the vast majority of eukaryotic genomes that we searched have at least one. A RUS protein from the fungal species *Coprinopsis cinerea* okayama7#130 has a predicted protein with an oxidoreductase enzyme fused in front of a DUF647 domain (XP_001838896). This is interesting because, in the over 50 RUS proteins we looked at from various species, it is the only example that has an additional predicted domain besides DUF647. This has perhaps been misannotated, as previously a mevalonate diphosphate decarboxylase-DUF647-fused protein was predicted in a *Neurospora* species, only later to be annotated as two separate proteins. Therefore, the overwhelming bulk of sequence data suggest that RUS proteins are made up primarily of the DUF647 domain. Additional parts of RUS proteins are typically small and nonconserved.

To analyze the phylogenetic relationships between RUS proteins, we performed a ClustalW alignment, which we then used to create a phylogenetic tree using maximum-likelihood point-accepted mutation with neighbor joining. For our analysis, we used protein sequences from Arabidopsis, rice, moss, the green algae *Ostreococcus lucimarinus*, human, mouse, zebrafish (zgc:162613), and *Drosophila* (CG10338). Interestingly, the RUS protein in animals clusters with AtRUS3 (At1g13770) from Arabidopsis, and the phylogeny constructed for RUS3 proteins mimics the phylogenetic relationship of these species. These data suggest that the plant RUS3 proteins are true orthologs of the RUS proteins in animal lineages. RUS1, RUS2, and RUS6 also have highly supported clades between the moss, rice, and Arabidopsis lineages, strongly supporting the orthology of these genes between these species. The RUS3 cluster is a monophyletic grouping within the larger RUS phylogeny, which suggests that there were several *RUS* genes in the ancestor of animals and plants and that only the *RUS3* ortholog has been maintained in animals. However, the base of the RUS family tree is only weakly defined, with very short branch lengths between groupings. Therefore, we cannot rule out that the additional *RUS* genes in plants are the result of early duplications in the plant kingdom. It is very likely, however, that the common ancestor of moss and higher plants had multiple *RUS* genes, as there is a clear orthological relationship between the moss RUS proteins and the rice and Arabidopsis RUS proteins. The *O. lucimarinus* genome has two *RUS* genes, one that clusters with RUS4 and another that does not clearly cluster with any of the RUS proteins from plants. Thus, RUS proteins exist in most plants and animals and in some fungi, but the basal relationships are not clearly definable. We conclude that the animal RUS protein has an ortholog in plants and that that ortholog is RUS3.

DISCUSSION

We have isolated and analyzed the *RUS2* gene, a second gene in addition to *RUS1* that when mutated gives a root UV-B-sensitive phenotype (Tong et al., 2008). Under our standard growth conditions, the *rus1* and *rus2* mutant plants display a virtually indistinguishable development-block phenotype that occurs after the seedling has emerged from the seed. Rather than being more severe, the double *rus1 rus2* mutant

has the same phenotype as either of the single mutants alone. Additionally, we have shown that the RUS1 and RUS2 proteins interact in a yeast two-hybrid assay via the DUF647 domain, a conserved domain in eukaryotes that both RUS1 and RUS2 share. RUS1 and RUS2 also share similar gene expression and GFP fluorescence patterns, supporting the hypothesis that they function together. RUS1 is predicted to be localized to plastids, and RUS2 has been empirically proposed to be in plastids in a previous study (Ferro et al., 2003). Interestingly, RUS2 does not have a clear subcellular signaling sequence, which suggests that RUS2 may be localized to the plastid as a consequence of its interaction with RUS1.

We have shown that like *rus1* mutants, *rus2* mutant plants are hypersensitive to light in the UV-B range (280–320 nm). *rus2-1* mutant roots are approximately 80% the length of wild-type plants when grown in the dark. As light increases, the roots become progressively shorter until they essentially fail to elongate at all in the full growth chamber light. We interpret these results to suggest that the RUS1/RUS2 complex acts as a negative modulator of a unique UV-B perception pathway in Arabidopsis. Without either RUS1 or RUS2, the small amount of UV-B present in the growth chamber lights is perceived by the plant as a much larger amount. It is unlikely that RUS1/RUS2 is involved in a UV-B-defensive pathway for several reasons. First, *rus1* and/or *rus2* mutant plants do not die in the light; they are merely blocked from developing, and they recover when the root is covered. If such a small amount of UV-B were causing severe damage to *rus* mutant plants, then it is logical to conclude that these plants would die after a few days. Second, the amount of UV-B needed to induce a strong *rus* phenotype is very low (<0.1 μmol m^{-2} s^{-1}) and is considered to be nondamaging at that level (Ulm and Nagy, 2005; Brown and Jenkins, 2008). Finally, the shoot phenotype of *rus1* and/or *rus2* mutants is ameliorated by reducing UV-B light reaching the root, suggesting that a root-to-shoot signal is involved in the shoot phenotype. If UV-B damages the shoot in *rus* mutants, covering the roots alone would not cause recovery of the shoot. For these reasons, we conclude that the *RUS1* and *RUS2* genes are involved in a novel UV-B signaling pathway, which when overstimulated in the roots causes a block to postgermination development.

Previous reports have focused on the role of *UVR8*, *HY5*, and *HYH* genes in regulating the response to UV-B in Arabidopsis (Ulm et al., 2004; Brown et al., 2005; Brown and Jenkins, 2008). A major focus of these studies was on the requirement of these transcription factors in the UV-B-induced expression of genes involved in UV-B protection. We previously showed *rus1* mutants to be capable of expressing UV-B-induced genes at a level comparable with the wild type (Tong et al., 2008). Thus, it does not appear to us that the RUS1/RUS2 pathway is involved in the UV-B protection pathways. Also, *rus1* and *rus2* plants do not appear to be affected in a DNA damage pathway, as the DNA damage-induced *BREAST CANCER SUSCEPTIBILITY1* (West et al., 2004) gene is not induced in *rus1* mutant plants at the low levels of UV-B used here. This suggests that DNA damage is not a cause of the *rus1/rus2* phenotypes (data not shown).

Based on the similar phenotypes of *rus1* and *rus2* mutants, we hypothesized that the proteins might interact physically in the same complex. RUS1 and RUS2 proteins did indeed interact in our yeast two-hybrid analysis. Additionally, the DUF647 domain of RUS1 was necessary and sufficient for this interaction. The region of RUS1 preceding the DUF647 domain did not interact with RUS2, and it is yet to be determined whether this region is required for RUS1 function. In vivo, these two proteins have indistinguishable localizations when analyzed via GFP fusion constructs. RUS1 is strongly predicted to be plastid localized, and RUS2, although not predicted to be plastid localized, has been previously found in a study that isolated plastid proteins (Ferro et al., 2003). *rus1 rus2* double mutants have the same phenotype as either of the single mutants alone. This suggests that the loss of one gene destroys the activity of the pathway, so that an additional loss of the other gene has no further effect. These data strongly support a model where RUS1 and RUS2 physically interact to perform their function(s) in the cell. Interaction of homologous proteins is a common occurrence in biological systems. One statistically based study showed that homologous proteins interact with each other at a rate higher than the rate of nonhomologous proteins (Orlowski et al., 2007). Thus, one possibility is that the heteromultimerization of RUS1 and RUS2 allowed for the fine-tuning of function of the complex that would not be possible with only a single RUS gene interacting with itself. In animals,

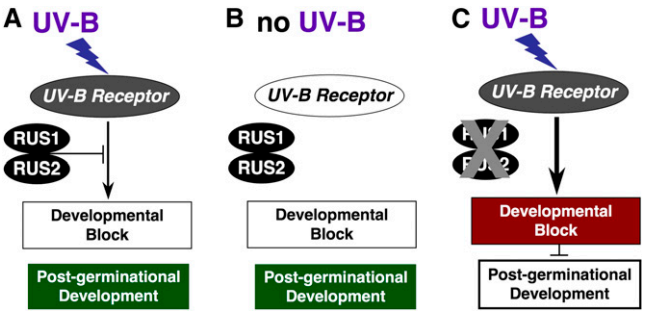

Figure 7. A working model explaining how RUS1 and RUS2 may function in root UV-B response during early seedling development. A, The wild-type condition. UV-B is perceived by a UV-B receptor, and the RUS1/RUS2 complex greatly diminishes the signal from the receptor to the developmental block response. B, The wild-type condition in the dark. Without UV-B, there is no signal sent from the UV-B receptor; thus, the RUS1/RUS2 complex becomes unnecessary. C, The *rus1*, *rus2*, or *rus1 rus2* mutant condition. Without the RUS1/RUS2 complex, the signal from the UV-B receptor is greatly increased and activates the developmental block response. [See online article for color version of this figure.]

there exists but a single *RUS* gene, which means that in animals RUS must work as a homomultimer if it requires a self-interaction for its function. Future work will focus on identifying the exact nature of the interaction between RUS1 and RUS2 and on identifying any additional members of the complex.

DUF647 proteins (RUS proteins) exist in many eukaryotic species, including all of the plants (Goff et al., 2002; Yu et al., 2002; Rensing et al., 2008; Swarbreck et al., 2008) and animals (except chicken) for which we have sufficient genomic sequence data, and also some fungi. Interestingly, the family of proteins is larger in individual plants than in the animals for which we had complete genomic sequences to analyze. Our phylogenetic analyses make it clear that the RUS proteins are more ancient than the plant/animal evolutionary split and that *RUS3* (*At1g13770*) in Arabidopsis is the *RUS* ortholog to the *RUS* genes in the animal lineages. The RUS proteins in animals clearly cluster with the RUS3 protein from Arabidopsis, suggesting that the function of this gene is conserved and highly important for all of these species. The moss and rice genomes have five orthologs each to the six Arabidopsis *RUS* genes, with a sixth gene in each lineage that is a clear lineage-specific duplication. Interestingly, although Arabidopsis is known to have undergone at least a partial autotetraploidization in the past, none of the *RUS* genes in Arabidopsis appears to be a lineage-specific duplication. RUS proteins are extremely important for Arabidopsis, as shown by the severe phenotypes of *rus1* and *rus2* mutants as well as *rus6/emb1879*, which is an embryo-lethal gene (www.seedgenes.org; Tzafrir et al., 2003). We are hopeful that our analysis of RUS proteins in Arabidopsis will also yield insight into the function of the animal RUS proteins and specifically the human RUS protein.

Our results strongly support a model where the *RUS1* and *RUS2* genes work together in the same genetic and biochemical pathway(s). In our model, RUS1 and RUS2 physically interact and are necessary to modulate a signal from a UV-B receptor negatively (Fig. 7A). This signal positively regulates a proposed "developmental block" that prevents further development after germination (Fig. 7A). The RUS1/RUS2 complex is required to dampen or diminish this signal under normal UV-B light quantities. In the dark or in a UV-B-free light environment, the receptor is not activated; thus, the action of the RUS1/RUS2 complex is not required (Fig. 7B). Without RUS1 or RUS2, the signal from the UV-B receptor is not properly dampened and is thus large enough to activate the post-germination developmental block (Fig. 7C). This model best represents our current understanding of our *rus* mutant data. *rus* mutant plants exhibit a hypersensitive response to LF or VLF UV-B, and our model represents this by placing the RUS1/RUS2 complex in a position to modulate the signal in this response.

Our model predicts that high levels of UV-B light will elicit a *rus*-like phenotype in wild-type plants. This is virtually impossible to test, however, as UV-B light at high fluence is very damaging, making it impossible to distinguish signaling responses from damage responses. This model also predicts that a loss of the receptor or of key signaling components would restore a wild-type phenotype to *rus* plants. Since there are currently no known photoreceptors for UV-B in plants, the *rus1* and *rus2* mutant phenotypes represent an opportunity for identifying the photoreceptor(s) responsible for perceiving low-level, nondamaging UV-B. Currently, we are focusing on identifying suppressors of *rus* mutants in Arabidopsis. Having a strong UV-B-induced phenotype under VLF UV-B should be ideal for identifying additional members of this UV-B perception pathway.

MATERIALS AND METHODS

Plant Material and Growth Conditions

Arabidopsis (*Arabidopsis thaliana* Col-0) plants were grown as described before (Lally et al., 2001). For petri dish-grown seedlings, surface-sterilized seeds were either cold treated at 4°C for at least 48 h or were without any cold treatment before being plated on MS growth medium (Murashige and Skoog, 1962) with 2% Suc on square plates (100 × 1,003 × 15 mm; Fisher Scientific) that were kept vertically in a growth chamber (Percival model CU36L5). For soil-grown plants, seeds with or without the 4°C cold treatment were directly sown in pots containing sterilized soil medium (Metro-Mix 220; Grace Sierra Horticultural Products) and kept in a growth chamber (Percival model AR-66L) with a 16-h-light/8-h-dark cycle at a constant temperature (23°C). White growth light was provided by cool-white fluorescence light tubes (Philips F17T8/TL741 for model CU36L5, Philips F32T8/TL741 for model AR-66L) and maintained at 100 μmol m^{-2} s^{-1}. For various light fluence levels, the following filters were used: Lee ND 298 (0.15, one-half stop), Lee ND 209 (0.3, one stop), Lee ND 210 (0.6, two stop), and Lee ND 299 (1.2, four stop; Lee Filters). Other light treatments were followed as described previously (Tong et al., 2008). For non-UV-B filters, a transparent plexiglass acrylic sheet (6 mm) was purchased from Ridout Plastics; for the UV filter, a 6-mm Photodyne UV filter was purchased from Spectronics. Light fluence measurements and spectral analyses were carried out using a Wideband Spectroradiometer (model RPS900-R) and its software (International Light).

Genetic Analysis and Gene Mapping

The *rus2* mutation segregates as a typical recessive allele. The ratio of wild type to *rus2* from the F1 parents is 3:1. *rus1 rus2* double mutants were created by crossing *rus2-1* to the three available *rus1* alleles (*rus1-1*, *rus1-2*, and *rus1-3*), and the double mutation was confirmed by known established markers. Genotyping analysis and a map-based approach were followed as described previously (Tong et al., 2008).

Confocal Microscopy

Seven-day-old seedlings were used for GFP detection. GFP fluorescence was excited by a blue argon laser (10 mW, 488-nm blue excitation) and detected at 515- to 530-nm wavelengths in a Nikon C1 Confocal E600FN microscope. Whole roots were directly mounted in water and observed with water objectives (203 and 603). Wild-type seedlings were used as negative controls. Images were processed and arranged by Adobe Photoshop version CS3.

Root Length Measurements

Vertically grown plates were photographed, and the images were analyzed using the ImageJ program (Rasband et al., 1997–2008; Abramoff et al., 2004; http://rsb.info.nih.gov/ij/). Root lengths were determined by measuring the length of a line traced along the root.

RT-PCR Analyses

RNA was extracted from plant tissues using the RNeasy Mini Kit (Qiagen catalog no. 74106) and quantified spectrophotometrically. Reverse transcriptase reactions were carried out using the OneStep RT-PCR Kit (Qiagen catalog no. 210210). The reactions were scaled down from 50 to 15 μL with all reagents kept at the same final concentrations. For each reaction, 100 ng of total extracted RNA was used. Reverse transcriptase reactions were done for 50 min at 50°C, followed by a 2-min 95°C step to activate the HotStarTaq DNA polymerase. The PCRs were done for 25 to 35 cycles, depending on the gene. The PCR temperatures and times were as follows: 30 s of denaturing at 94°C; 30 s of annealing at 52°C; and 1 min of extension at 72°C. The reaction products were run on 2% agarose gels and imaged using a Kodak 4000R Image Station. Products were sequenced to confirm identity. Primer sequences and cycle numbers are available upon request.

Yeast Two-Hybrid Analysis

Yeast two-hybrid analysis was performed using the vectors from the Matchmaker Two-Hybrid Library and Construction Kit (Clontech catalog no. 630445). cDNAs were cloned into either pGADT7 or pGBKT7 and transformed into yeast to create yeast containing a single vector. Yeast were mated together to create yeast with two vectors for two-hybrid analysis. Confirmation of the presence of both vectors was performed by growing the yeast on medium lacking Trp and Leu. Experimental protein-protein interaction was determined by growth on plates lacking Trp, Leu, and His and containing 5-Bromo-4-chloro-3-indolyl-α-D-galactoside. Vectors provided by the Matchmaker Kit were used as controls. For control experiments, yeast were generated with the pGADT7-Rec plasmid and either the pGBKT7-53 or the pGBKT7-Lam vector for positive and negative controls, respectively.

Phylogenetic Analysis

Proteins were aligned using the ClustalW program. The BLOSUM30 matrix was used for pair-wise alignment with an open gap penalty of 10 and an extend gap penalty of 0.1. Multiple alignment was performed using the BLOSUM Series with an open gap penalty of 10, an extend gap penalty of 0.05, and a delay divergent of 40%. Trees were constructed using the PHYLIP phylogenetic analysis programs. Trees were constructed using Protdist with point-accepted mutation settings, followed by the Neighbor program for neighbor-joining analysis. For bootstrap analysis, the Seqboot program was used prior to the Protdist and Neighbor programs, followed by the Consensus program to create a consensus tree. A total of 1,000 samples were used for bootstrapping. Trees were drawn with the Drawtree program.

Sequence data from this article can be found in the GenBank/EMBL data libraries under accession numbers NP_609897.2 (DmRUS), NP_001103923.1 (DrRUS), Q91W34.1 (MmRUS), NP_073581.1 (HsRUS), XP_001419164.1 (OlRUSA), XP_001418386.1 (OlRUSB), XP_001755448.1 (PpRUS1), XP_001766030.1 (PpRUS2), XP_001764017.1 (PpRUS3), XP_001759421.1 (PpRUS4), XP_001762143.1 (PpRUS6A), XP_001764974.1 (PpRUS6B), CAE02373.2 (OsRUS1), NP_001053319.1 (OsRUS2), ABF94623.1 (OsRUS3), NP_001041984.1 (OsRUS5), BAD82242.1 (OsRUS6A), NP_190175.2 (AtRUS1), NP_565718.1 (AtRUS2), NP_172832.3 (AtRUS3), NP_179928.2 (AtRUS4), NP_195771.2 (AtRUS5), and NP_568713.1 (AtRUS6/EMB1879).

ACKNOWLEDGMENTS

We are very grateful to Winslow Briggs (Carnegie Institute of Washington, Stanford, CA) for critically reading the manuscript and for helpful discussions. We thank members of the He laboratory for discussions and Annette Chan (Cell Molecular Imaging Center, San Francisco State University, San Francisco) for help with the confocal microscopy.

Received March 30, 2009; accepted June 6, 2009; published June 10, 2009.

LITERATURE CITED

Abramoff MD, Magelhaes PJ, Ram SJ (2004) Image processing with ImageJ. Biophotonics International **11:** 36–42

Arabidopsis Genome Initiative (2000) Analysis of the genome sequence of the flowering plant *Arabidopsis thaliana*. Nature **408:** 796–815

Bae G, Choi G (2008) Decoding of light signals by plant phytochromes and their interacting proteins. Annu Rev Plant Biol **59:** 281–311

Ballare CL, Scopel AL, Stapleton AE, Yanovsky MJ (1996) Solar ultraviolet-B radiation affects seedling emergence, DNA integrity, plant morphology, growth rate, and attractiveness to herbivore insects in *Datura ferox*. Plant Physiol **112:** 161–170

Brown BA, Cloix C, Jiang GH, Kaiserli E, Herzyk P, Kliebenstein DJ, Jenkins GI (2005) A UV-B-specific signaling component orchestrates plant UV protection. Proc Natl Acad Sci USA **102:** 18225–18230

Brown BA, Jenkins GI (2008) UV-B signaling pathways with different fluence-rate response profiles are distinguished in mature Arabidopsis leaf tissue by requirement for UVR8, HY5, and HYH. Plant Physiol **146:** 576–588

Caldwell MM, Bjorn LO, Bornman JF, Flint SD, Kulandaivelu G, Teramura AH, Tevini M (1998) Effects of increased solar ultraviolet radiation on terrestrial ecosystems. J Photochem Photobiol B **46:** 40–52

Cashmore AR, Jarillo JA, Wu YJ, Liu D (1999) Cryptochromes: blue light receptors for plants and animals. Science **284:** 760–765

Christie JM (2007) Phototropin blue-light receptors. Annu Rev Plant Biol **58:** 21–45

DeYoung BJ, Clark SE (2001) Signaling through the CLAVATA1 receptor complex. Plant Mol Biol **46:** 505–513

Emanuelsson O, Nielsen H, Brunak S, von Heijne G (2000) Predicting subcellular localization of proteins based on their N-terminal amino acid sequence. J Mol Biol **300:** 1005–1016

Eppig JT, Blake JA, Bult CJ, Kadin JA, Richardson JE, and the Mouse Genome Database Group (2007) The Mouse Genome Database (MGD): new features facilitating a model system. Nucleic Acids Res **35:** D630–D637

Ferro M, Salvi D, Brugière S, Miras S, Kowalski S, Louwagie M, Garin J, Joyard J, Rolland N (2003) Proteomics of the chloroplast envelope membranes from *Arabidopsis thaliana*. Mol Cell Proteomics **2:** 325–345

Fritsche E, Schäfer C, Calles C, Bernsmann T, Bernshausen T, Wurm M, Hübenthal U, Cline JE, Hajimiragha H, Schroeder P, et al (2007) Lightening up the UV response by identification of the arylhydrocarbon receptor as a cytoplasmatic target for ultraviolet B radiation. Proc Natl Acad Sci USA **104:** 8851–8856

Frohnmeyer H, Staiger D (2003) Ultraviolet-B radiation-mediated responses in plants balancing damage and protection. Plant Physiol **133:** 1420–1428

Garinis GA, Mitchell JR, Moorhouse MJ, Hanada K, de Waard H, Vandeputte D, Jans J, Brand K, Smid M, van der Spek PJ, et al (2005) Transcriptome analysis reveals cyclobutane pyrimidine dimers as a major source of UV-induced DNA breaks. EMBO J **24:** 3952–3962

Goff SA, Ricke D, Lan TH, Presting G, Wang R, Dunn M, Glazebrook J, Sessions A, Oeller P, Varma H, et al (2002) A draft sequence of the rice genome (*Oryza sativa* L ssp *japonica*). Science **296:** 92–100

Horton P, Park KJ, Obayashi T, Fujita N, Harada H, Adams-Collier CJ, Nakai K (2007) WoLF PSORT: protein localization predictor. Nucleic Acids Res **35:** W585–W587

Horton P, Park KJ, Obayashi T, Nakai K (2006) Protein subcellular localization prediction with WoLF PSORT. *In* T Jiang, U-C Yang, Y-PP Chen, L Wong, eds, Proceedings of the 4th Annual Asia Pacific Bioinformatics Conference. Imperial College Press, London, pp 39–48

Ispolatov I, Yuryev A, Mazo I, Maslov S (2005) Binding properties and evolution of homodimers in protein-protein interaction networks. Nucleic Acids Res **33:** 3629–3635

Kim BC, Tennessen DJ, Last RL (1998) UV-B-induced photomorphogenesis in *Arabidopsis thaliana*. Plant J **15:** 667–674

Konieczny A, Ausubel FM (1993) A procedure for mapping Arabidopsis mutations using co-dominant ecotype-specific PCR-based markers. Plant J **4:** 403–410

Koornneef M, Dellaert LWM, van der Veen JH (1982) EMS- and radiation-induced mutation frequencies at individual loci in *Arabidopsis thaliana* (L.) Heynh. Mutat Res **93:** 109–123

Lally D, Ingmire P, Tong HY, He ZH (2001) Antisense expression of a cell wall-associated protein kinase, WAK4, inhibits cell elongation and alters morphology. Plant Cell **13:** 1317–1331

Lao K, Glazer AN (1996) Ultraviolet-B photodestruction of a light-harvesting complex. Proc Natl Acad Sci USA **93:** 5258–5263

Li J, Ou-Lee TM, Raba R, Amundson RG, Last RL (1993) *Arabidopsis*

flavonoid mutants are hypersensitive to UV-B irradiation. Plant Cell **5:** 171–179

Liscum E, Hodgson DW, Campbell TJ (2003) Blue light signaling through the cryptochromes and phototropins: so that's what the blues is all about. Plant Physiol **133:** 1429–1436

Liu YG, Huang N (1998) Efficient amplification of insert end sequences from bacterial artificial chromosome clones by thermal asymmetric interlaced PCR. Plant Mol Biol Rep **16:** 175–181

McKenzie RL, Bjorn LO, Bais A, Ilyasd M (2003) Changes in biologically active ultraviolet radiation reaching the Earth's surface. Photochem Photobiol Sci **2:** 5–15

Murashige T, Skoog F (1962) A revised medium for rapid growth and bioassays with tobacco tissue cultures. Physiol Plant **15:** 473–497

Nogues S, Allen DJ, Morison JIL, Baker NR (1999) Characterization of stomatal closure caused by ultraviolet-B radiation. Plant Physiol **121:** 489–496

Oravecz A, Baumann A, Máté Z, Brzezinska A, Molinier J, Oakeley EJ, Ádám É, Schäfer E, Nagy F, Ulm R (2006) CONSTITUTIVELY PHOTOMORPHOGENIC1 is required for the UV-B response in *Arabidopsis*. Plant Cell **18:** 1975–1990

Orlowski J, Kaczanowski S, Zielenkiewicz P (2007) Overrepresentation of interactions between homologous proteins in interactomes. FEBS Lett **581:** 52–56

Quail PH, Boylan MT, Parks BM, Short TW, Xu Y, Wagner D (1995) Phytochromes: photosensory perception and signal transduction. Science **268:** 675–680

Rasband WS (1997–2008) Image J. National Institutes of Health, Bethesda, MD. http://rsb.info.nih.gov//ij (April 16, 2008)

Rensing SA, Lang D, Zimmer AD, Terry A, Salamov A, Shapiro H, Nishiyama T, Perroud PF, Lindquist EA, Kamisugi Y, et al (2008) The *Physcomitrella* genome reveals evolutionary insights into the conquest of land by plants. Science **319:** 64–69

Riechmann JL, Krizek BA, Meyerowitz EM (1996) Dimerization specificity of *Arabidopsis* MADS domain homeotic proteins APETELA1, APETELA3, and AGAMOUS. Proc Natl Acad Sci USA **93:** 4793–4798

Ries G, Buchholz G, Frohnmeyer H, Hohn B (2000) UV-damage-mediated induction of homologous recombination in *Arabidopsis* is dependent on photosynthetically active radiation. Proc Natl Acad Sci USA **97:** 13425–13429

Russinova E, Borst JW, Kwaaitaal M, Cano-Delgado A, Yin Y, Chory J, de Vries SC (2004) Heterodimerization and endocytosis of Arabidopsis brassinosteriod receptors BRI1 and AtSERK3 (BAK1). Plant Cell **16:** 3216–3229

Smith H (1999) Tripping the light fantastic. Nature **400:** 710–712

Steinmüller D, Tevini M (1985) Action of ultraviolet radiation (UV-B) upon cuticular waxes in some crop plants. Planta **164:** 557–564

Suesslin C, Frohnmeyer H (2003) An *Arabidopsis* mutant defective in UV-B light-mediated responses. Plant J **33:** 591–601

Swarbreck D, Wilks C, Lamesch P, Berardini TZ, Garcia-Hernandez M, Foerster H, Li D, Meyer T, Muller R, Ploetz L, et al (2008) The Arabidopsis Information Resource (TAIR): gene structure and function annotation. Nucleic Acids Res **36:** D1009–D1014

Taylor JS, Raes J (2004) Duplication and divergence: the evolution of new genes and old ideas. Annu Rev Genet **38:** 615–643

Tong H, Leasure CD, Hou X, Yuen G, Briggs W, He ZH (2008) Role of root UV-B sensing in *Arabidopsis* early seedling development. Proc Natl Acad Sci USA **105:** 21039–21044

Tzafrir I, Dickerman A, Brazhnik O, Nguyen Q, McElver J, Frye C, Patton D, Meinke D (2003) The Arabidopsis SeedGenes project. Nucleic Acids Res **31:** 90–93

Ulm R, Baumann A, Oravecz A, Máté Z, Ádám É, Oakeley EJ, Schäfer E, Nagy F (2004) Genome-wide analysis of gene expression reveals function of the bZIP transcription factor HY5 in the UV-B response of *Arabidopsis*. Proc Natl Acad Sci USA **101:** 1397–1402

Ulm R, Nagy F (2005) Signalling and gene regulation in response to ultraviolet light. Curr Opin Plant Biol **8:** 477–482

Ulmasov T, Hagen G, Guilfoyle TJ (1999) ARF1, a transcription factor that binds to auxin response elements. Science **276:** 1865–1868

Walterscheid JP, Nghiem DX, Kazimi N, Nutt LK, McConkey DJ, Norval M, Ullrich SE (2006) *Cis*-urocanic acid, a sunlight-induced immunosuppressive factor, activates immune suppression via the 5-HT2A receptor. Proc Natl Acad Sci USA **105:** 17420–17425

Waterworth WM, Jiang Q, West CE, Nikaido WM, Bray CM (2002) Characterization of *Arabidopsis* photolyase enzymes and analysis of their role in protection from ultraviolet-B radiation. J Exp Bot **53:** 1005–1015

West CE, Waterworth WM, Sunderland PA, Bray CM (2004) Arabidopsis DNA double-strand break repair pathways. Biochem Soc Trans **32:** 964–966

Whitelam GC, Halliday KJ, editors (2007) Light and Plant Development: Annual Plant Reviews, Vol 30. Wiley, Hoboken, NJ

Wilson IW, Ghosh S, Gerhardt KE, Holland N, Babu TS, Edelman M, Dumbroff EB, Greenberg BM (1995) In vivo photomodification of ribulose-1,5-bisphosphate carboxylase/oxygenase holoenzyme by ultraviolet-B radiation. Plant Physiol **109:** 221–229

Yu J, Hu S, Wang J, Wong GK, Li S, Liu B, Deng Y, Dai L, Zhou Y, Zhang X, et al (2002) A draft sequence of the rice genome (*Oryza sativa* L ssp *indica*). Science **296:** 79–92

Zimmermann P, Hirsch-Hoffmann M, Hennig L, Gruissem W (2004) GENEVESTIGATOR: Arabidopsis microarray database and analysis toolbox. Plant Physiol **136:** 2621–2632